

DETC2009-87525

A FREQUENCY DOMAIN FINITE ELEMENT APPROACH FOR THREE-DIMENSIONAL GEAR DYNAMICS

Christopher G. Cooley

Dynamics and Vibrations Lab
Department of Mechanical Engineering
The Ohio State University
Columbus, OH 43210
Email: cooley.168@osu.edu

Robert G. Parker*

State Key Lab for Mechanical
Systems and Vibration
University of Michigan - SJTU Joint Institute
Shanghai Jiao Tong University
Shanghai, China
Email: parker.242@osu.edu

Sandeep M. Vijayakar

Advanced Numerical Solutions
Hilliard, OH 43026
Email: sandeep@ansol.com

ABSTRACT

A finite element formulation for the dynamic response of gear pairs is proposed. Following an established approach in lumped parameter gear dynamic models, the static transmission error is used as the excitation in a frequency domain solution of the finite element vibration model. The nonlinear finite element/contact mechanics formulation provides superior calculation of static transmission error and average mesh stiffness that is used in the dynamic simulation. The frequency domain finite element calculation of dynamic response correlates to numerically integrated (time domain) finite element dynamic results and previously published experimental results. Simulation time with the proposed formulation is two orders of magnitude lower than numerically integrated dynamic results. This formulation admits system level dynamic gearbox response, which may include multiple gear meshes, flexible shafts, rolling element bearings, and housing structures.

INTRODUCTION

Gear vibration is transferred to the surrounding structure by shafts and bearings, creating unwanted noise. Dynamic tooth loads at or near resonant gear speeds cause high stresses in the teeth and bearings and can cause premature failure. For these reasons the dynamic behavior of gears is essential to the proper design of geared systems.

Although gear dynamics has been studied for decades, few studies present a formulation intended for full gear-train systems that contain multiple gear meshes, flexible shafts, bearings, and housing structures. There are few reliable computational tools for the dynamic analysis of general gear configurations. Some models exist, but they are limited by poor modeling of gear tooth mesh interface, two-dimensional models that neglect out-of-plane behavior, and specific models for a single gear configuration. General three-dimensional finite element models are a rarity because they require significant computational effort for dynamic response. In multi-body dynamic simulations, many time steps are required for the transient response to diminish so that steady state data can be obtained. This study attempts to fill this gap with a general finite element formulation that can be used for full gearbox dynamic analyses.

A linear approach that uses the static transmission error as excitation is proposed. The use of static transmission error as excitation is common in gear dynamics modeling [5, 11, 13, 19]. This work offers superior static transmission error calculation from a nonlinear, three-dimensional finite element/contact mechanics formulation. The static transmission error is then used as excitation to a linear finite element model of a gear pair. The variations from tooth compliance or profile modifications are determined at multiple locations over a mesh cycle. Spur and helical gears are handled naturally by this formulation.

This formulation is examined for single gear pairs as a benchmark. Both spur and helical gears are examined. Compar-

*Address all correspondence to this author.

isons are made to numerically integrated (time domain) finite element solutions and experimental data found in the literature. This method works well for off-resonance regimes for highly nonlinear spur gears and in all regimes for helical gear pairs. Additionally, the new formulation brings computational efficiency to general three-dimensional gear dynamics. This method allows system level dynamic analyses for gear transmission systems in reasonable times.

Typical analyses model gear dynamics using lumped parameter models. These models commonly assume the gear blanks to be rigid bodies with lumped spring elements to model the gear mesh interface. The complexity of the gear mesh interface varies for each model. Accurate gear mesh modeling is essential to capturing the dynamics of gears, and lumped parameter models suffer due to the various approximations made in modeling the gear mesh interface. A review of gear dynamic models can be found in [14].

Lumped parameter mesh models for helical gears are more complex than the single lumped stiffness element used for spur gears. Some models use many lumped stiffness elements that are placed along the discretized contact lines of a helical gear. Blankenship and Singh review the mathematical models used for gear mesh interfaces [2] and develop a general three-dimensional formulation for gear pairs in [3,4]. Kahraman [5] investigated the dynamics of a helical gear pair using a single stiffness element to represent each tooth pair in mesh. He found the helix angle had little effect on the natural frequency of a helical gear pair, and, for helix angles less than twenty degrees, a spur gear model gives reasonable results for natural frequency.

Experimental studies by Kahraman and Blankenship showed the existence of nonlinear response in spur gears [6–9]. Additionally, they experimentally investigated the effect of contact ratio and tooth profile modifications on spur gear dynamics.

Recently, a finite element/contact mechanics approach has been used to study the dynamic properties of gears [15, 16, 18]. All dynamic results so far have been restricted to two-dimensional analyses that assume plane strain behavior of the gears in mesh. Parker et al. showed the ability of a two-dimensional finite element/contact mechanics formulation to accurately capture the strongly nonlinear dynamics of spur gear pairs [16]. The model was able to predict the nonlinear jump-up and jump-down frequencies and amplitude of resonant response accurately as compared to experiments. This formulation was shown to predict more accurate nonlinear behavior over simple single degree-of-freedom models. The major advantage of the finite element/contact mechanics approach is that no restrictions or assumptions about the gear mesh interface are made and the contact forces are calculated at each instant as the gears move kinematically. Parker et al. used the same formulation in [16] to study the dynamic response of a two-dimensional planetary gear train model [15]. The finite element/contact mechanics formulation has been used successfully in many other studies related to gear stress and dynamics, for example [1, 10, 12, 17].

FINITE ELEMENT ANALYSIS

Time Domain Finite Element/Contact Mechanics Formulation

Parker et al. [16] gives the detailed mathematics for the two-dimensional finite element/contact mechanics formulation for gear dynamics. This work extends the same formulation to three dimensions. The formulation of the three-dimensional finite element approach is similar to the two-dimensional case. Therefore, only an overview is provided here and the details can be found in [16].

The equations of motion for an arbitrary single gear body i can be written as

$$\begin{bmatrix} \mathbf{M}_{ffi} & \mathbf{M}_{fri} \\ \mathbf{M}_{fri}^T & \mathbf{M}_{rri} \end{bmatrix} \begin{pmatrix} \ddot{\mathbf{x}}_{fi} \\ \ddot{\mathbf{x}}_{ri} \end{pmatrix} + \begin{bmatrix} \mathbf{C}_{ffi} & \mathbf{C}_{fri} \\ \mathbf{C}_{fri}^T & \mathbf{C}_{rri} \end{bmatrix} \begin{pmatrix} \dot{\mathbf{x}}_{fi} \\ \dot{\mathbf{x}}_{ri} \end{pmatrix} + \begin{bmatrix} \mathbf{K}_{ffi} & \mathbf{K}_{fri} \\ \mathbf{K}_{fri}^T & \mathbf{K}_{rri} \end{bmatrix} \begin{pmatrix} \mathbf{x}_{fi} \\ \mathbf{x}_{ri} \end{pmatrix} = \begin{pmatrix} \mathbf{f}_{fi} \\ \mathbf{f}_{ri} \end{pmatrix} \quad (1)$$

where \mathbf{M}_{ffi} and \mathbf{K}_{ffi} are the finite element mass and stiffness matrices, respectively. The vector \mathbf{x}_{fi} contains the finite element degrees of freedom, and the vector \mathbf{x}_{ri} contains the six rigid body degrees of freedom of the i^{th} gear reference frame. The damping matrix is found using a Rayleigh damping model, $\mathbf{C}_{ffi} = \alpha\mathbf{M}_{ffi} + \beta\mathbf{K}_{ffi}$. Any added lumped mass or inertia is placed in \mathbf{M}_{rri} . Stiffness and damping terms from a lumped element bearing model are added to \mathbf{K}_{rri} and \mathbf{C}_{rri} . The off-diagonal matrices couple the elastic and rigid body degrees of freedom.

Assembling the equations of motion for each gear into a single matrix equation gives

$$\mathbf{M}\ddot{\mathbf{x}} + \mathbf{C}\dot{\mathbf{x}} + \mathbf{K}\mathbf{x} = \mathbf{f} \quad (2)$$

Equation (2) is solved using a time discretization method. After discretization, Equation (2) can be written in the compact form

$$\hat{\mathbf{K}}\hat{\mathbf{x}} = \hat{\mathbf{f}} \quad (3)$$

where

$$\hat{\mathbf{K}} = \mathbf{M} + \gamma\Delta t\mathbf{C} + \beta\Delta t^2\mathbf{K}$$

$$\hat{\mathbf{f}} = -[-2\mathbf{M} + (1 - 2\gamma)\Delta t\mathbf{C} + (\frac{1}{2} - 2\beta + \gamma)\Delta t^2\mathbf{K}]\mathbf{x}_n - [\mathbf{M} - (1 - \gamma)\Delta t\mathbf{C} + (\frac{1}{2} + \beta - \gamma)\Delta t^2\mathbf{K}]\mathbf{x}_{n-1} + \Delta t^2[\beta\mathbf{f}_{n+1} + (\frac{1}{2} - 2\beta + \gamma)\mathbf{f}_n + (\frac{1}{2} + \beta - \gamma)\mathbf{f}_{n-1}] \quad (4)$$

$$\mathbf{x}_n = \mathbf{x}(t_o + n\Delta t)$$

$$\mathbf{f}_n = \mathbf{f}(t_o + n\Delta t).$$

The discretization parameters β and γ are chosen to give numerical stability without adding damping. We can think of $\hat{\mathbf{K}}$ and $\hat{\mathbf{f}}$ in Equations (3) and (4) as the effective stiffness matrix and forcing vector. The unknown dynamic solution vector at time $t_o + (n + 1)\Delta t$ is given by $\hat{\mathbf{x}} = \mathbf{x}_{n+1}$.

The response vector, $\hat{\mathbf{x}}$, is broken up by a linear transformation that separates the elastic (\mathbf{q}_ϕ) and rigid body (\mathbf{q}_θ) degrees of freedom according to

$$\hat{\mathbf{x}} = \mathbf{T} \begin{pmatrix} \mathbf{q}_\phi \\ \mathbf{q}_\theta \end{pmatrix} \quad (5)$$

where the matrix \mathbf{T} contains the eigenvectors of the symmetric matrix $\hat{\mathbf{K}}$.

Substitution of Equation (5) into (3) and premultiplying by the transpose of \mathbf{T} breaks the matrix equation of motion into two separate equations, one that leads to the displacement equation for the gear tooth interface and one that gives a force balance equation for the gear bodies. These two equations are used to solve the contact problem at the gear mesh interface.

The contact modeling is the highlight of the finite element/contact mechanics formulation. A combined finite element and semi-analytical formulation (a surface integration of the Bousinesq solution for a point load on an elastic half-space) is used to model the contact between the gear teeth [20–22]. A detailed overview can be found in [15, 16] as applied to gear dynamics. A brief overview is given below.

The separation due to external and contact loading is written as

$$\mathbf{d} = \mathbf{A}\mathbf{p} + \mathbf{C}\mathbf{q}_\theta + \boldsymbol{\epsilon} \quad (6)$$

where \mathbf{A} is a compliance matrix that gives the contribution of the inner (semi-analytical) and outer (finite element) contribution to separation from contact, \mathbf{p} is a vector of contact loads, \mathbf{C} is a kinematic matrix that adds the rigid body contribution to separa-

tion, \mathbf{q}_θ is a vector of rigid body degrees of freedom, and $\boldsymbol{\epsilon}$ is the contribution to separation from finite element deformations due to external loading.

The forces on the finite element mesh are balanced by

$$\mathbf{C}^T\mathbf{p} = \boldsymbol{\lambda} \quad (7)$$

where $\boldsymbol{\lambda}$ is the transformed external force vector.

Equations (6) and (7) are solved by linear programming methods [21] for each element of \mathbf{d} and \mathbf{p} subject to the constraints that each of the k components, $d_k, p_k \geq 0$ and one (but not both) of d_k and p_k are zero for every k . The calculated \mathbf{d} and \mathbf{p} are then used to find the finite element displacement vector, $\hat{\mathbf{x}}$.

The main limitation of a full three-dimensional finite element dynamic simulation is the computational cost of running such a model. Because this is a multi-body dynamic formulation a full gear model is used, and the gear pair is kinematically rotating during the analysis. Additionally, a number of computation steps are required to remove the transient response. These two areas, which are crucial to the dynamic finite element simulation, consume much computation time.

Frequency Domain Finite Element/Contact Mechanics Formulation

The frequency domain method begins by finding the gear tooth mesh stiffness and static transmission error by static simulations at many points over a mesh cycle. For a static simulation the time derivatives of \mathbf{x} in Equation (2) are set to zero, leaving

$$\mathbf{K}\mathbf{x} = \mathbf{f} \quad (8)$$

Equation (8) is in the same form as Equation (3) and is solved in exactly the same way. The results from the foregoing time domain formulation apply with Equation (8) in place of Equation (3).

Equations (6) and (7) give components of \mathbf{d} and \mathbf{p} , each of which contains positive or zero elements with nonzero entries in \mathbf{p} corresponding to zero entries in \mathbf{d} . If we partition \mathbf{p}_b to contain all nonzero entries of \mathbf{p} , then the corresponding elements of \mathbf{d}_b will be zero. The partitioned equation of (6) is then written as

$$\mathbf{d}_b = \mathbf{0} = \mathbf{A}_{bb}\mathbf{p}_b + \mathbf{C}_b\mathbf{q}_\theta + \boldsymbol{\epsilon}_b \quad (9)$$

Solution of (9) for \mathbf{p}_b gives

$$\mathbf{p}_b = -\mathbf{A}_{bb}^{-1} \mathbf{C}_b \mathbf{q}_\theta - \mathbf{A}_{bb}^{-1} \boldsymbol{\epsilon}_b \quad (10)$$

In general, \mathbf{A}_{bb} is a large matrix and calculation of its inverse is computationally intensive. This is not the case, however, because \mathbf{A}_{bb}^{-1} is calculated during the linear programming solution of \mathbf{d} and \mathbf{p} from Equation (6) and (7). Therefore, \mathbf{A}_{bb}^{-1} is available with no additional computations.

Substitution of (10) into the basic partition of (7) and rearranging gives

$$\mathbf{K}_{qq} \mathbf{q}_\theta = \boldsymbol{\lambda} + \boldsymbol{\lambda}_\epsilon \quad (11)$$

where $\mathbf{K}_{qq} = \mathbf{C}_b^T \mathbf{A}_{bb}^{-1} \mathbf{C}_b$ and $\boldsymbol{\lambda}_\epsilon = -\mathbf{C}_b^T \mathbf{A}_{bb}^{-1} \boldsymbol{\epsilon}_b$.

Equation (11) represents the contact stiffness of the gear mesh interface. The matrix \mathbf{K}_{qq} is the time varying (as the gears rotate) contact stiffness matrix with respect to the rigid body degrees of freedom in \mathbf{q}_θ . The second forcing term in (11), $\boldsymbol{\lambda}_\epsilon$, is the excitation that occurs due to tooth surface modifications and vanishes for gear teeth that have no modifications.

Because Equation (11) is a stiffness matrix that depends on the contact conditions as the gears rotate kinematically through a mesh cycle, multiple steps are analyzed over a mesh period. The mesh cycle is divided into N steps and a corresponding \mathbf{K}_{qq} is found at each step. This mesh stiffness depends only on the position in the mesh cycle and is transformed into a time dependent stiffness $\mathbf{K}_{qq}(t)$ using the mesh frequency. The static displacement vector \mathbf{x}_s is found at each of the N steps and is transformed using the mesh frequency to give $\mathbf{x}_s(t)$.

Using static condensation to eliminate certain degrees of freedom and Guyan reduction of the mass and damping matrices in Equation (2) (the stiffness matrix is unchanged by the Guyan reduction) gives

$$\hat{\mathbf{M}} \ddot{\mathbf{q}}^* + \hat{\mathbf{C}} \dot{\mathbf{q}}^* + \hat{\mathbf{L}} \mathbf{q}^* = \hat{\mathbf{f}} \quad (12)$$

where

$$\begin{aligned} \hat{\mathbf{M}} &= (\mathbf{T}\mathbf{W})^T \mathbf{M} \mathbf{T}\mathbf{W} & \hat{\mathbf{C}} &= (\mathbf{T}\mathbf{W})^T \mathbf{C} \mathbf{T}\mathbf{W} \\ \hat{\mathbf{L}} &= (\mathbf{T}\mathbf{W})^T \mathbf{K} \mathbf{T}\mathbf{W} & \hat{\mathbf{f}} &= (\mathbf{T}\mathbf{W})^T \mathbf{f} \\ \mathbf{x} &= \mathbf{T}\mathbf{W} \begin{pmatrix} \mathbf{q}_\phi^* \\ \mathbf{q}_\theta^* \end{pmatrix} = \mathbf{T}\mathbf{W} \mathbf{q}^* \end{aligned} \quad (13)$$

where $(\cdot)^*$ indicates the degrees of freedom retained during static condensation. The matrix \mathbf{W} is the transformation matrix from the static condensation process that relates the retained degrees

of freedom to the removed degrees of freedom.

The stiffness matrix $\hat{\mathbf{L}}$ does not contain mesh stiffness from gear tooth contact and has components

$$\hat{\mathbf{L}} = \begin{bmatrix} \hat{\mathbf{K}}_{\phi\phi} & \mathbf{0} \\ \mathbf{0} & \mathbf{0} \end{bmatrix} \quad (14)$$

Augmenting Equation (14) with the stiffness due to contact ($\mathbf{K}_{qq}(t)$) found from the nonlinear semi-analytical formulation leaves the mass and damping matrices unchanged, but the stiffness equation becomes

$$\hat{\mathbf{L}} = \begin{bmatrix} \hat{\mathbf{K}}_{\phi\phi} & \mathbf{0} \\ \mathbf{0} & \mathbf{K}_{qq}(t) \end{bmatrix} \quad (15)$$

The mesh stiffness associated with the contact can be broken into mean and time varying parts, $\mathbf{K}_{qq}(t) = \bar{\mathbf{K}}_{qq} + \tilde{\mathbf{K}}_{qq}(t)$. The stiffness matrix $\hat{\mathbf{K}}_{\phi\phi}$ does not change with time. The stiffness matrix is also decomposed into mean and time varying parts, $\hat{\mathbf{L}} = \hat{\mathbf{K}}_m + \hat{\mathbf{K}}_v(t)$. With the addition of contact stiffness, these are

$$\hat{\mathbf{K}}_m = \begin{bmatrix} \hat{\mathbf{K}}_{\phi\phi} & \mathbf{0} \\ \mathbf{0} & \bar{\mathbf{K}}_{qq} \end{bmatrix} \quad \hat{\mathbf{K}}_v(t) = \begin{bmatrix} \mathbf{0} & \mathbf{0} \\ \mathbf{0} & \tilde{\mathbf{K}}_{qq}(t) \end{bmatrix} \quad (16)$$

Substitution of the stiffness matrices in Equation (16) into Equation (12) gives

$$\hat{\mathbf{M}} \ddot{\mathbf{q}}^* + \hat{\mathbf{C}} \dot{\mathbf{q}}^* + (\hat{\mathbf{K}}_m + \hat{\mathbf{K}}_v(t)) \mathbf{q}^* = \hat{\mathbf{f}} \quad (17)$$

Equation (17) is a linear time varying equation of motion for the geared system with time varying mesh stiffness. This equation is not in the ideal form for a finite element solution. Therefore, the time varying stiffness term is brought to the right-hand side giving

$$\hat{\mathbf{M}} \ddot{\mathbf{q}}^* + \hat{\mathbf{C}} \dot{\mathbf{q}}^* + \hat{\mathbf{K}}_m \mathbf{q}^* = \hat{\mathbf{f}} - \hat{\mathbf{K}}_v(t) \mathbf{q}^* \quad (18)$$

To solve (18) the right-hand side of the equation is approximated as follows to get a linear time-invariant system of equations. If we assume the dynamic contribution to the tooth forces is small, the static and dynamic tooth forces will be equal. This means that $\hat{\mathbf{M}} \ddot{\mathbf{q}}^*$ and $\hat{\mathbf{C}} \dot{\mathbf{q}}^*$ in Equation (17) are small compared to the other terms. Neglecting them gives

$$\left(\hat{\mathbf{K}}_m + \hat{\mathbf{K}}_v(t)\right) \mathbf{q}^* = \hat{\mathbf{f}} \quad (19)$$

Equation (19) has the static solution $\mathbf{q}^* = \mathbf{q}_s^*$. Rearranging, the approximation for the RHS of Equation (18) becomes

$$\hat{\mathbf{f}} - \hat{\mathbf{K}}_v(t)\mathbf{q}_s^* = \hat{\mathbf{K}}_m\mathbf{q}_s^* \quad (20)$$

Substitution of the approximation in Equation (20) into Equation (18) gives the final approximate equation for the dynamic response of the system

$$\hat{\mathbf{M}}\ddot{\mathbf{q}} + \hat{\mathbf{C}}\dot{\mathbf{q}} + \hat{\mathbf{K}}_m\mathbf{q} = \hat{\mathbf{K}}_m\mathbf{q}_s \quad (21)$$

The eigenvalue problem associated with Equation (21) comes from the homogeneous solution with the assumed harmonic displacement $\mathbf{q} = \mathbf{Q}e^{j\omega t}$

$$-\omega^2\hat{\mathbf{M}}\mathbf{Q} + \hat{\mathbf{K}}_m\mathbf{Q} = \mathbf{0} \quad (22)$$

Equation (22) is solved by conventional methods for the gear system natural frequencies (ω_n) and mode shapes (\mathbf{Q}_n). Equation (21) represents a forced linear oscillator. The forcing term, $\hat{\mathbf{K}}_m\mathbf{q}_s$, is repeated as each tooth passes through the gear mesh interface and contains frequency components at integer multiples of the tooth mesh frequency f_m . Typically, only a few harmonics of mesh frequency are used in the analysis because the Fourier coefficients of the higher harmonics of static transmission error are negligible compared to the first few. Generally 3-5 terms are used in the dynamic calculation. More or less terms can be added as necessary.

RESULTS AND DISCUSSION

Three-Dimensional Spur Gear Dynamics

Time Domain Analysis. The gear pairs analyzed in this study are those from an experimental investigation into the nonlinear dynamics of spur gear pairs conducted by Kahraman and Blankenship [7, 9]. The gears have 3 mm module, 20° pressure angle, and both have 50 teeth. The reference diameter is 150 mm, the base diameter is 140.98 mm, and the circular tooth thickness is 4.64 mm. Both the pinion and gear have the same geometry other than the outside diameter, which is varied to give different involute contact ratios (ICR). The outside diameters to achieve

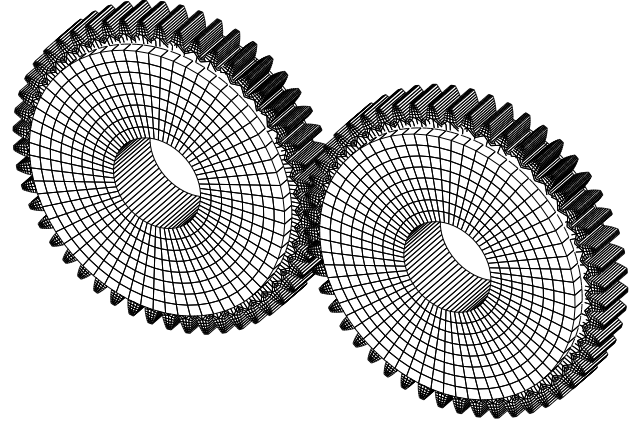


Figure 1. FINITE ELEMENT MODEL OF A SPUR GEAR PAIR.

a 1.37 ICR are 154.4 and 154.7 mm for the pinion and gear, respectively. To get a 1.77 ICR the pinion and gear have 156.04 and 156.08 mm outer diameters, respectively. Figure 1 shows the finite element mesh of the spur gear model used in the dynamic simulations.

The natural frequency is found from a numerical impulse test. The gears are brought to rest at zero speed at a specified torque then loaded impulsively with 1.2 times this nominal torque for a single integration step. The next step brings the gears back to operational torque. The resulting transients are analyzed to find the natural frequency and damping in the spur gear pair. Spur gears will have two distinct natural frequencies for one and two tooth contact (assuming the the contact ratio is between one and two). To obtain a single natural frequency, the two values are averaged according to the contact ratio by $f_n = (2 - \text{ICR})f_1 + (\text{ICR} - 1)f_2$, where f_1 and f_2 are the natural frequencies of the gear pair with one and two teeth in contact, respectively.

The time domain finite element calculation of natural frequency for the ICR 1.37 gear pair at 170 N-m torque gives 2457 Hz and 3011 Hz for one and two teeth in contact, respectively. The average natural frequency is 2662 Hz, within 3% of the experimentally reported natural frequency in [7].

The dynamic response of a gear pair is found by running the time domain simulation at a specified speed while the transient response diminishes. After the transients are gone, the steady state data is recorded over a number of mesh cycles. The vibration is quantified by the dynamic transmission error (DTE) defined as $DTE = r_1\theta_1 + r_2\theta_2$, where r_1 and r_2 are the base radii and θ_1 and θ_2 are the rotational deflections of the gear and pinion. To change between two fixed speeds, the gears are slowly accelerated over a number of mesh cycles to not introduce numerical instabilities into the solution.

The dynamic response of a unity ratio spur gear pair with ICR of 1.37 is shown in Figure 2 at 170 N-m torque. The gears are operated for a wide range of mesh frequencies and the nonlin-

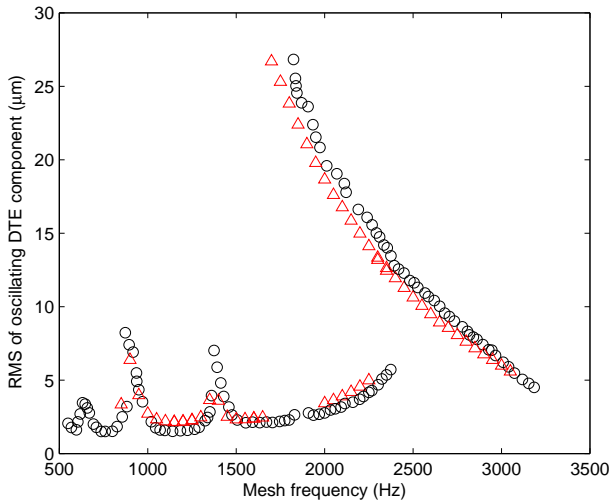


Figure 2. TIME DOMAIN FINITE ELEMENT CALCULATION OF RMS OF OSCILLATING DYNAMIC TRANSMISSION ERROR FOR A THREE-DIMENSIONAL SPUR GEAR PAIR WITH ICR 1.37 AT 170 N-m TORQUE (Δ) COMPARED TO EXPERIMENTAL DATA FROM [7] (\circ).

ear response is shown for the primary resonance ($f_m \approx f_n$) and excitation at higher harmonics ($f_m \approx f_n/l$ for integer $l > 1$). The finite element results accurately capture the dynamics of the gear pair as compared to the experimental data in [7]. The response shows the well-known softening type nonlinearity, where the backbone of the nonlinear response at the primary resonance bends toward the left as the large amplitude vibration causes tooth separation [7, 16]. The jump frequencies are identified and match the experimental data.

While the ability to capture the strongly nonlinear three-dimensional spur gear dynamics with contact loss is encouraging, the analysis takes a great deal of time. It takes approximately five hours to analyze one mesh frequency on a conventional dual-core computer. Considering one typically wants to find the response over a wide range of mesh frequencies, a typical analysis may consist of 20 or more mesh frequencies. To capture the nonlinear response, increasing and decreasing speed sweeps are analyzed, requiring a total of 40 mesh frequencies. This gives a total of 200 hours of computation time. With this kind of time investment, the time domain finite element formulation is not practical in most cases. Additionally, this is only for a spur gear pair, meaning this method of solution is not feasible for a system level analysis where multiple gears are coupled together with shafts, bearings, and a housing.

Frequency Domain Analysis. To avoid the long calculation time using the time domain formulation, the linear frequency domain method is adopted. Considerable time savings are obtained from this method as only a static simulation with a

relatively few number of time steps are needed to solve for both the natural frequencies and dynamic response. For comparison, three simulations are needed if the time domain solution is used, two for the impulse tests (for one and two tooth pairs in contact) to find the natural frequency and a speed sweep to find the dynamic response around the resonance. These simulations total thousands of time steps and many hours of computation. The frequency domain method only requires a static analysis over one mesh cycle, which typically totals 20-30 steps. This section shows the effectiveness of this approach, which uses static transmission error as excitation to approximate gear pair dynamic behavior as described earlier.

Table 1 shows the frequency domain finite element calculation of natural frequency as compared to experimental results in [7, 9]. The natural frequency is predicted accurately by the frequency domain method for each torque, with 7.08% as the highest percent difference. The natural frequency predicted by the time domain finite element formulation is 2662 Hz for the ICR 1.37 spur gear pair at 170 N-m torque. There is less than 0.1% difference between the time domain and frequency domain finite element results for natural frequency.

Table 1. FREQUENCY DOMAIN FINITE ELEMENT CALCULATION OF NATURAL FREQUENCY (Hz) FOR A UNITY RATIO SPUR GEAR PAIR WITH ICR 1.37 AND 1.77 FOR 85, 170 AND 340 N-m TORQUE.

	85 N-m	170 N-m	340 N-m
ICR 1.37			
Frequency domain			
finite element	2592	2664	2728
Experimental [7, 9]	2620	2740	2880
Percent difference	1.07%	2.81%	5.42%
ICR 1.77			
Frequency domain			
finite element	2780	2800	2860
Experimental [7, 9]	2700	2900	3070
Percent difference	2.92%	3.51%	7.08%

Figure 3 shows the finite element calculation of static transmission error over one mesh cycle and its spectra for the spur gear pairs with ICR 1.37 and 1.77 at 85, 170, and 340 N-m torque. The magnitude of each harmonic gives an idea of the relative amount of forcing to the gear pair and gives a qualitative picture of what to expect in the dynamic response.

Figures 4 and 5 show the frequency domain finite element calculation of dynamic response as compared to experimental

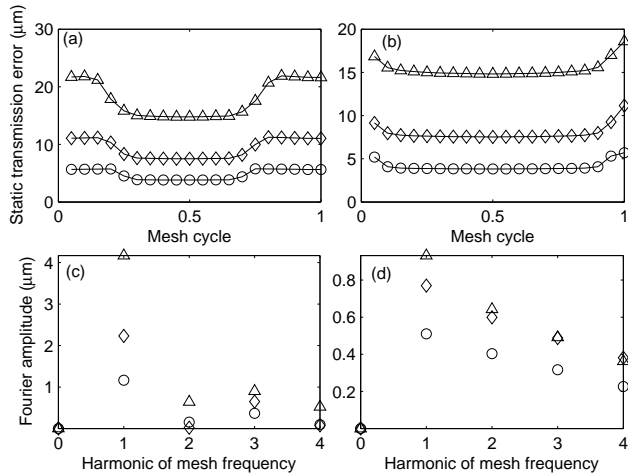


Figure 3. FINITE ELEMENT CALCULATION OF STATIC TRANSMISSION ERROR AND SPECTRA (MEAN REMOVED) FOR A THREE-DIMENSIONAL ICR 1.37 (a,c) AND 1.77 (b,d) SPUR GEAR PAIR FOR 85 N-m (○), 170 N-m (◇), AND 340 N-m (△) TORQUE.

data in [7, 9] for 1.37 and 1.77 contact ratio spur gear pairs at varying torque. Figures (a), (b), and (c) are for 85, 170, and 340 N-m torque for each contact ratio. The resonant frequencies at the natural frequency and higher harmonics are predicted accurately by the frequency domain method for both contact ratios at varying torques (also seen in the natural frequency results in Table 1). The off-resonant amplitudes of dynamic response correlate well with the experimental data. Amplitudes at resonance, however, do not correlate well with experiments due to the strong nonlinear behavior for this lightly damped gear set. Nonlinear phenomena cannot be captured by the proposed frequency domain solution because the linear formulation is based on the assumption the static tooth forces approximate the dynamic tooth forces. This is a poor assumption for large amplitude vibration. In such cases, especially with tooth contact loss deviations from the frequency domain method and nonlinear gear response are expected.

The overall correlation in Figures 4 and 5 is positive. The natural frequency and off-resonant regimes are predicted accurately. Additionally, resonances due to excitations with higher harmonics are captured.

The resonance regimes for more highly damped gear systems may yield better correlation from the diminished amplitude and less contact loss. The experimental gear test stand was intentionally built with light damping. Gears used in industry may have more damping that would be better predicted using the proposed method.

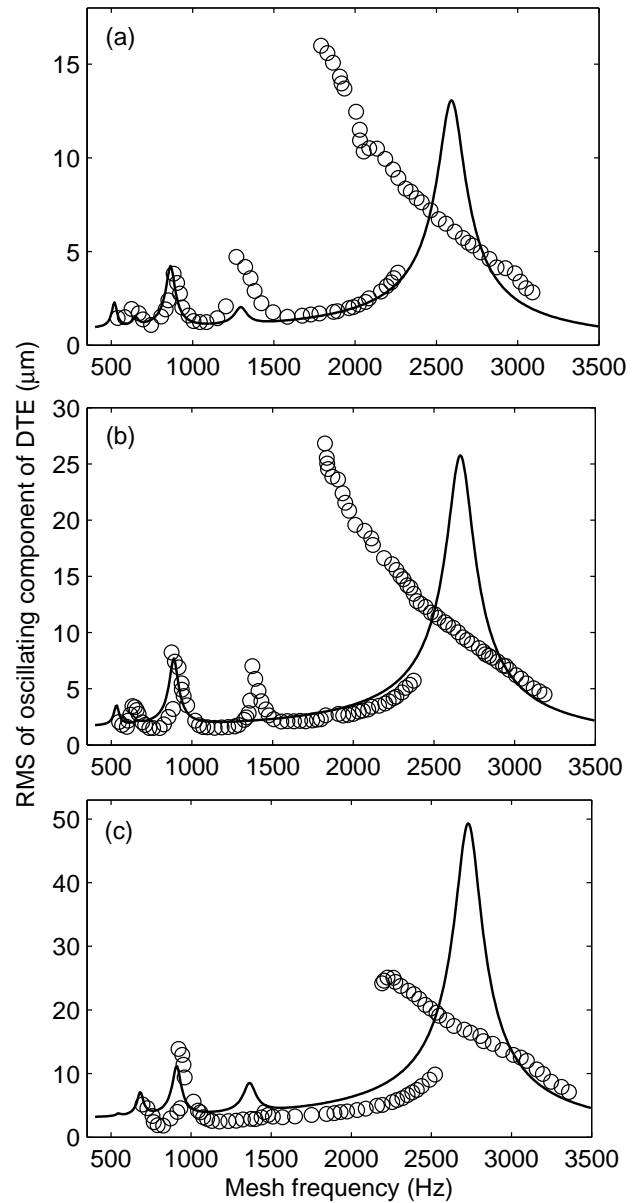


Figure 4. FREQUENCY DOMAIN FINITE ELMEENT CALCULATION OF RMS OF DYNAMIC TRANSMISSION ERROR FOR A THREE-DIMENSIONAL ICR 1.37 SPUR GEAR PAIR (SOLID) AS COMPARED TO EXPERIMENTAL DATA FROM [7,9] (○) AT 85 (a), 170 (b), AND 340 (c) N-m TORQUE.

Three-Dimensional Helical Gear Dynamics

Nonlinear tooth contact loss is not common in moderately to heavily loaded helical gear pairs [5]. Because of the smooth tooth mesh action from the helix angle, a constant mesh stiffness can be used in lumped parameter helical gear models [5, 19]. For these two reasons the frequency domain method should perform

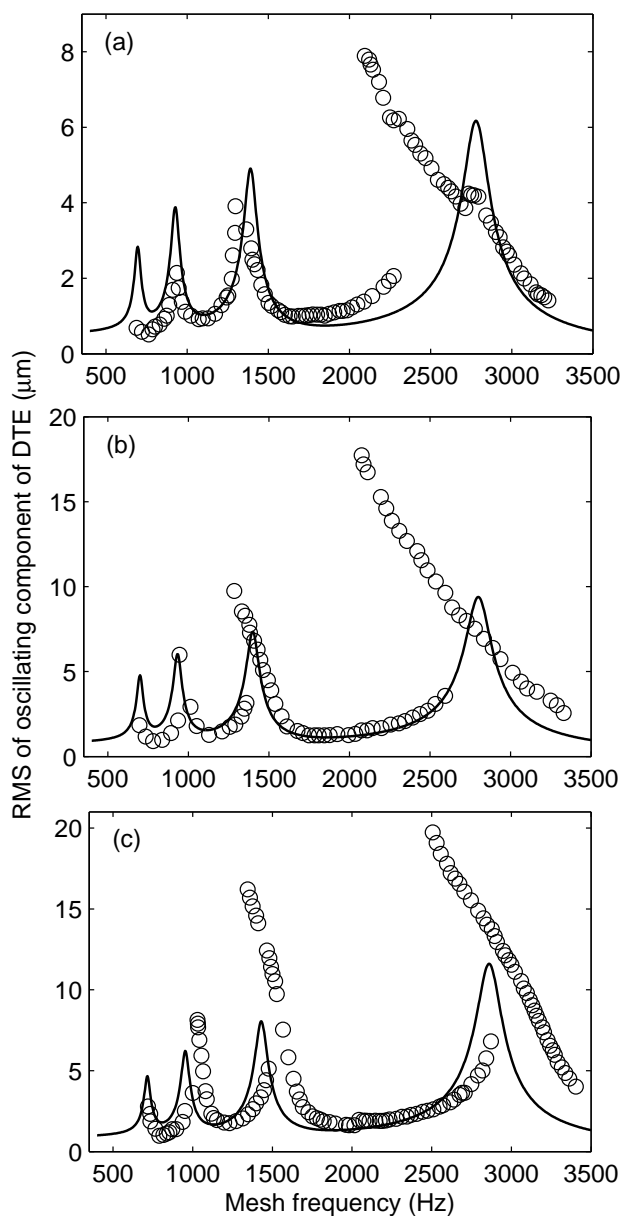


Figure 5. FINITE ELMEENT CALCULATION OF RMS OF DYNAMIC TRANSMISSION ERROR FOR A THREE-DIMENSIONAL ICR 1.77 SPUR GEAR PAIR (SOLID) AS COMPARED TO EXPERIMENTAL DATA FROM [7,9] (○) AT 85 (a), 170 (b), AND 340 (c) N-m TORQUE.

best for these systems. As seen previously, the formulation captures the dynamic response well except at resonance, where non-linear tooth contact loss occurs. For helical gear models without tooth contact loss the agreement should be better than that for nonlinear spur gears.

The geometric properties of the helical gear pair used in this study are the same as those for the ICR 1.37 spur gear pair except

for the addition of a helix angle. Two helix angles are investigated, 15° and 30° . These two helix angles represent the maximum helix angle (because of geometry constraints) and the minimum helix angle without contact loss occurring. Similar to the spur gear analyses, the helical gears are mounted on stiff shafts, rendering a torsional dynamic model of helical gear vibration.

A time domain finite element numerical impulse test gives the natural frequency of the profile ICR 1.37 helical gear pair with a 30° helix angle as 1582 Hz. The frequency domain finite element formulation gives 1593 Hz natural frequency, a 0.7% difference compared to the time domain calculation.

Figure 6 shows a comparison of the finite element calculation of dynamic response as calculated by the time and frequency domain methods for a profile ICR 1.37 helical gear pair with 30° helix angle at 170 N-m torque. The frequency domain solution accurately predicts the dynamic response compared to the benchmark time domain solution, including at the higher harmonic excitation zones near 791 Hz and 527 Hz. The time domain simulation in this case took four days to analyze, whereas the frequency domain method took less than one hour.

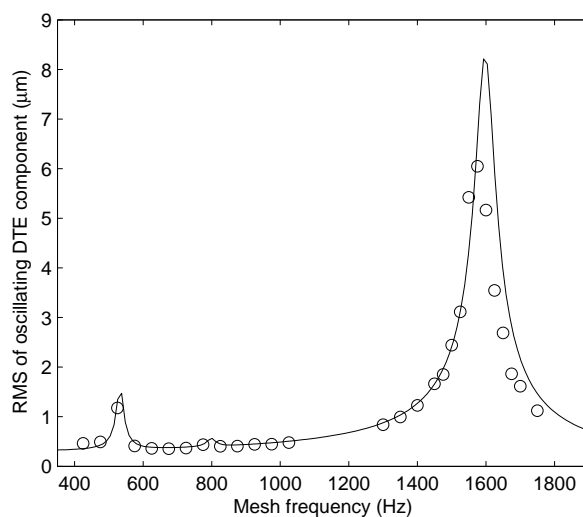


Figure 6. FINITE ELEMENT CALCULATION OF RMS OF DYNAMIC TRANSMISSION ERROR FOR A THREE-DIMENSIONAL PROFILE ICR 1.37 HELICAL GEAR PAIR WITH 30° HELIX ANGLE AT 170 N-m TORQUE. TIME DOMAIN SOLUTION (○) AND FREQUENCY DOMAIN SOLUTION (SOLID).

Figure 7 shows the finite element time and frequency domain calculation for dynamic response of a profile ICR 1.37 gear pair with a 15° helix angle on bearings represented by linear stiffness and damping elements. The gears are loaded to 170 N-m torque. The bearings are identical lumped element stiffness bearings with equal radial stiffnesses in both translation directions of

30×10^6 N/mm, axial stiffness of 10×10^6 N/mm, and 100×10^9 N-mm/rad in both tilting directions. Bearing damping is added to give 3.3% modal damping at the primary resonance. As compared to the 30° helix angle gear pair whose dynamic response is shown in Figure 6, the natural frequency has increased with a decrease in helix angle despite the added bearing compliance. Additionally, the RMS amplitude of response has increased. The strong correlation of the frequency domain results with the time domain solution remains for the decreased helix angle on lumped element stiffness bearings.

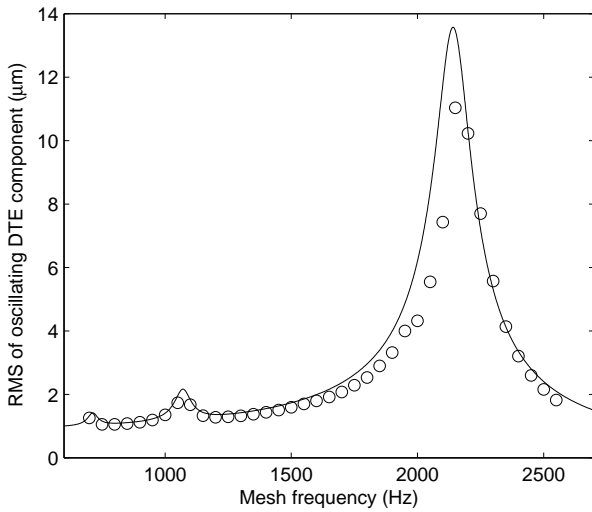


Figure 7. TIME DOMAIN (○) AND FREQUENCY DOMAIN (SOLID) FINITE ELEMENT CALCULATION OF RMS OF DYNAMIC TRANSMISSION ERROR FOR A THREE-DIMENSIONAL PROFILE ICR 1.37 HELICAL GEAR PAIR WITH 15° HELIX ANGLE AT 170 N-m TORQUE.

The frequency domain methods fast solution time is ideal for parameter studies. Figure 8 shows the change in static transmission error over one mesh cycle with torque for the 30° helix angle gear pair. Each torque shows nearly uniform deflection over a mesh cycle. The spectra of the static transmission errors indicate that the first harmonic for 340 N-m is roughly twice that of 170 N-m, and the first harmonic of 170 N-m is nearly twice that of 85 N-m. Figure 9 shows the dynamic response for the profile ICR 1.37 helical gear pair at 85 N-m and 340 N-m torque on rigid bearings. As the torque is increased, the response at the primary resonance increases with the same proportions found in the static transmission error. The natural frequency changes less than 6% between each torque.

Figure 10 shows the effect of helix angle on the natural frequency of a profile ICR 1.37 unity ratio and a nonunity ratio gear pair on rigid bearings. The gear pair natural frequencies decreases monotonically with increasing helix angle for both

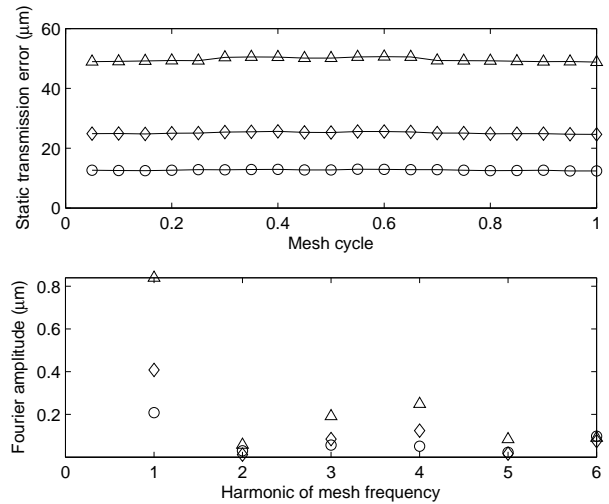


Figure 8. FINITE ELEMENT CALCULATION OF STATIC TRANSMISSION ERROR (UPPER) AND SPECTRA (MEAN REMOVED) (LOWER) FOR A THREE-DIMENSIONAL PROFILE ICR 1.37 HELICAL GEAR PAIR FOR 85 N-m (○), 170 N-m (◇), and 340 N-m (△) TORQUE.

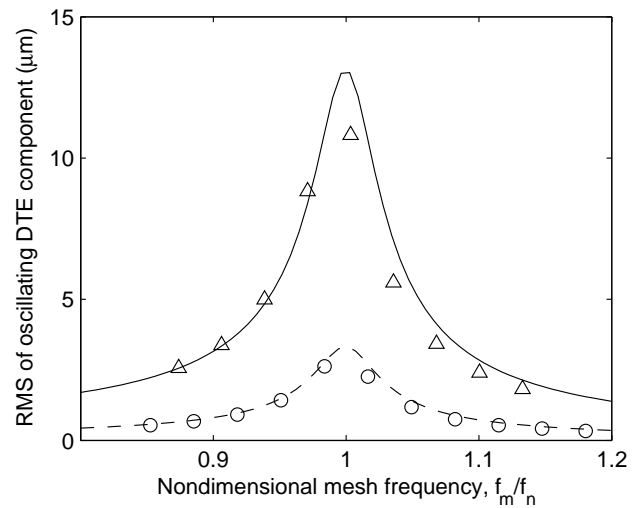


Figure 9. FINITE ELEMENT CALCULATION OF RMS OF DYNAMIC TRANSMISSION ERROR FOR A THREE-DIMENSIONAL PROFILE ICR 1.37 HELICAL GEAR PAIR WITH 30° HELIX ANGLE AT 85 N-m (DASHED - FREQUENCY DOMAIN SOLUTION, CIRCLES - TIME DOMAIN SOLUTION) AND 340 N-m (SOLID - FREQUENCY DOMAIN SOLUTION, TRIANGLES - TIME DOMAIN SOLUTION) TORQUE.

gear pairs. The difference in natural frequency of the unity ratio gear pair between the time and frequency domain methods from $0^\circ - 15^\circ$ helix angles is due to the time domain impulse test being analyzed at one location in the mesh cycle. In this range of helix angles there is a significant difference in mesh stiffness over a

mesh cycle. It is expected that helix angles less than 15° lead to nonlinear behavior due to the increased variation in mesh stiffness. Nonlinear behavior can be determined by comparing the natural frequency from a time domain impulse test and the frequency domain solution. If a difference in natural frequency is found, nonlinear behavior is expected in the dynamic response. Conversely, agreement of the two natural frequencies implies the response is linear. This could be useful for system level models where an increasing and decreasing speed sweep over a resonance may not be possible with conventional computers but numerical impulse tests are possible. The unity ratio gear pair with 15° and 30° helix angles has linear dynamic response and is accurately modeled by the frequency domain method as shown in Figures 6, 7, and 9.

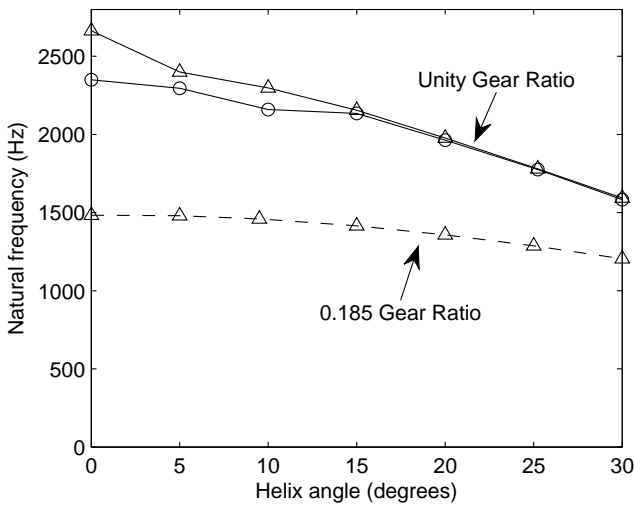


Figure 10. FINITE ELEMENT CALCULATION OF NATURAL FREQUENCY FOR A PROFILE ICR 1.37 GEAR PAIR WITH UNITY RATIO (SOLID) AT 170 N-m TORQUE AND A GEAR PAIR WITH NONUNITY RATIO (DASHED) WITH VARYING HELIX ANGLE BY THE TIME DOMAIN METHOD (○) AND THE FREQUENCY DOMAIN METHOD (△).

CONCLUSIONS

A computationally efficient frequency domain formulation for gear dynamics has been developed. The finite element/contact mechanics formulation accurately predicts the dynamic response of multiple three-dimensional spur and helical gear pairs. The main conclusions are:

1. The time domain finite element/contact mechanics formulation accurately models the strongly nonlinear dynamic behavior of lightly damped spur gear pairs in three-

dimensions. The analyses require significant computation time and are not suited for system level models.

2. The frequency domain method accurately predicts spur gear dynamic response for low to moderate amplitude vibration. Agreement in off-resonant amplitudes was shown for multiple contact ratios and torques as compared to experimental data and time domain finite element data.
3. The frequency domain method is well suited for the dynamic analysis of helical gears, where the nonlinearity due to contact loss is weaker than for spur gears. Dynamic response at resonant and off-resonant speeds are accurately captured using the frequency domain method with much less computational effort than the time domain solution.
4. The time savings of the frequency domain method could be used to dynamically model complete gearbox systems. These models could include multiple gear meshes, flexible shafts, rolling element bearings, and housing structures.

REFERENCES

- [1] V. K. Ambarisha and R. G. Parker. Nonlinear dynamics of planetary gears using analytical and finite element models. *Journal of Sound and Vibration*, 302(3):577–595, May 2007.
- [2] G. W. Blankenship and R. Singh. A comparative study of selected gear mesh interface dynamic models. In *ASME Design Engineering Technical Conferences, Biennial Conference on Mechanical Vibration and Noise*, Phoenix, Arizona, September 1992.
- [3] G. W. Blankenship and R. Singh. Dynamic force transmissibility in helical gear pairs. *Mechanism and Machine Theory*, 30(3):323–339, April 1995.
- [4] G. W. Blankenship and R. Singh. A new gear mesh interface dynamic model to predict multi dimensional force coupling and excitation. *Mechanism and Machine Theory*, 30(1):43–57, January 1995.
- [5] A. Kahraman. Effect of axial vibrations on the dynamics of a helical gear pair. *Journal of Vibration and Acoustics*, 115(1):33–39, January 1993.
- [6] A. Kahraman and G. W. Blankenship. Experiments on nonlinear dynamic behavior of an oscillator with clearance and periodically time-varying parameters. *Journal of Applied Mechanics*, 64(1):217–226, March 1997.
- [7] A. Kahraman and G. W. Blankenship. Effect of involute contact ratio on spur gear dynamics. *Journal of Mechanical Design*, 121(5):313–315, June 1999.
- [8] A. Kahraman and G. W. Blankenship. Effect of involute tip relief on dynamic response of spur gear pairs. *Journal of Mechanical Design*, 121(1):112–118, March 1999.
- [9] A. Kahraman and G. W. Blankenship. Gear dynamics experiments: Part ii: Effect of involute contact ratio. *ASME Power Transmission and Gearing Conference, San Diego*, 1996.

- [10] A. Kahraman, A. A. Kharazi, and M. Umrani. A deformable body dynamic analysis of planetary gears with thin rims. *Journal of Sound and Vibration*, 262:752–768, 2003.
- [11] A. Kahraman and R. Singh. Non-linear dynamics of a spur gear pair. *Journal of Sound and Vibration*, 142(1):49–75, October 1990.
- [12] A. Kahraman and S. M. Vijayakar. Effect of internal gear flexibility on the quasi-static behavior of a planetary gear set. *Journal of Mechanical Design*, 123(3):408–415, September 2001.
- [13] H. N. Ozguven and D. R. Houser. Dynamic analysis of high speed gears by using loaded static transmission error. *Journal of Sound and Vibration*, 125(1):71–83, August 1988.
- [14] H. N. Ozguven and D. R. Houser. Mathematical models used in gear dynamics – a review. *Journal of Sound and Vibration*, 121:383–411, 1988.
- [15] R. G. Parker, V. Agashe, and S. M. Vijayakar. Dynamic response of a planetary gear system using a finite element/contact mechanics model. *Journal of Mechanical Design*, 122(3):304–310, September 2000.
- [16] R. G. Parker, S. M. Vijayakar, and T. Imajo. Non-linear dynamic response of a spur gear pair: Modelling and experimental comparisons. *Journal of Sound and Vibration*, 237(3):435–455, October 2000.
- [17] Avinash Singh. Influence of planetary needle bearings on the performance of single and double pinion planetary systems. *Journal of Mechanical Design*, 129:85–94, January 2007.
- [18] V. K. Taminana, A. Kahraman, and S. M. Vijayakar. A study of the relationship between the dynamic factors and the dynamic transmission error of spur gear pairs. *Journal of Mechanical Design*, 129:75–84, January 2007.
- [19] P. Velex and M. Ajmi. On the modelling of excitations in geared systems by transmission errors. *Journal of Sound and Vibration*, 290(3-5):882–909, March 2006.
- [20] S. M. Vijayakar. A combined surface integral and finite-element solution for a three-dimensional contact problem. *International Journal for Numerical Methods in Engineering*, 31(3):525–545, March 1991.
- [21] S. M. Vijayakar, H. R. Busby, and D. R. Houser. Linearization of multibody frictional contact problems. *Computers and Structures*, 29(4):569–576, 1988.
- [22] S. M. Vijayakar, H. R. Busby, and Lowell Wilcox. Finite element analysis of three-dimensional conformal contact with friction. *Computers and Structures*, 33(1):49–61, 1989.